SCIENCE CHINA
Life Sciences

•RESEARCH PAPER•

December 2020 Vol.63 No.12: 1887–1894
https://doi.org/10.1007/s11427-018-1585-8

Finite element analysis of trans-lamina cribrosa pressure difference on optic nerve head biomechanics: the Beijing Intracranial and Intraocular Pressure Study

Yingyan Mao[1,2†], Diya Yang[2†], Jing Li[1,2], Jun Liu[3], Ruowu Hou[4], Zheng Zhang[2], Yiquan Yang[1,2], Lei Tian[1,2], Robert N. Weinreb[5] & Ningli Wang[1,2*]

[1]*Beijing Institute of Ophthalmology, Beijing Tongren Hospital, Capital Medical University, Beijing 100005, China;*
[2]*Beijing Ophthalmology and Visual Sciences Key Laboratory, Beijing Tongren Eye Center, Beijing Tongren Hospital, Capital Medical University, Beijing 100054, China;*
[3]*Department of Ophthalmology, The Ohio State University, Columbus 43210, USA;*
[4]*Department of Neurosurgery, Beijing Tongren Hospital, Capital Medical University, Beijing 100005, China;*
[5]*Hamilton Glaucoma Center and Department of Ophthalmology, University of California-San Diego, La Jolla, California 92093, USA*

Received August 9, 2019; accepted September 20, 2019; published online May 20, 2020

The present study aims to assess the potential difference of biomechanical response of the optic nerve head to the same level of trans-lamina cribrosa pressure difference (TLCPD) induced by a reduced cerebrospinal fluid pressure (CSFP) or an elevated intraocular pressure (IOP). A finite element model of optic nerve head tissue (pre- and post-laminar neural tissue, lamina cribrosa, sclera, and pia mater) was constructed. Computed stresses, deformations, and strains were compared at each TLCPD step caused by reduced CSFP or elevated IOP. The results showed that elevating TLCPD increased the strain in optic nerve head, with the largest strains occurring in the neural tissue around the sclera ring. Relative to a baseline TLCPD of 10 mmHg, at a same TLCPD of 18 mmHg, the pre-laminar neural tissue experienced 11.10% first principal strain by reduced CSFP and 13.66% by elevated IOP, respectively. The corresponding values for lamina cribrosa were 6.09% and 6.91%. In conclusion, TLCPD has a significant biomechanical impact on optic nerve head tissue and, more prominently, within the pre-laminar neural tissue and lamina cribrosa. Comparatively, reducing CSFP showed smaller strain than elevating IOP even at a same level of TLCPD on ONH tissue, indicating a different potential role of low CSFP in the pathogenesis of glaucoma.

cerebrospinal fluid pressure, glaucomatous optic neuropathy, laminar cribrosa, trans-laminar cribrosa pressure difference

Citation: Mao, Y., Yang, D., Li, J., Liu, J., Hou, R., Zhang, Z., Yang, Y., Tian, L., Weinreb, R.N., and Wang, N. (2020). Finite element analysis of trans-lamina cribrosa pressure difference on optic nerve head biomechanics: the Beijing Intracranial and Intraocular Pressure Study. Sci China Life Sci 63, 1887–1894. https://doi.org/10.1007/s11427-018-1585-8

INTRODUCTION

Glaucoma, a leading cause of irreversible vision loss, is characterized by loss of retinal ganglion cells (RGC) and their axons. The optic nerve head (ONH), lamina cribrosa (LC) in particular, is the principal site of RGC axonal insult in glaucoma. In addition, the LC is a discontinuity ("weak spot") in the corneo-scleral shell, which gives rise to stress or strain concentrations in the mechanical system. When considering LC biomechanics, it is natural to focus on the role of intraocular pressure (IOP), since it directly acts on the ONH and generates an outward force (Geijssen, 1991). However, the LC is also acted upon by the sclera, whose deformation is

†Contributed equally to this work
*Corresponding author (email: wningli@vip.163.com)

controlled not only by IOP but also by subarachnoid space pressure which is principally determined by intracranial cerebrospinal fluid pressure (CSFP) (Jonas et al., 2003; Morgan et al., 2002; Liu et al., 2019).

Recognizing this fact, several investigators have suggested that trans-lamina cribrosa pressure difference (TLCPD), which has been defined as IOP minus CSFP, may be more important for the pathophysiology of the ONH including the development of glaucomatous optic neuropathy. (Morgan et al., 2008; Berdahl et al., 2008; Ren et al., 2011; Wang et al., 2012). For example, in our previous experiments, monkeys with an artificially reduced CSFP and a resultant increased TLCPD developed damages of the optic nerve (Yang et al., 2014). We have also showed in a rat experimental model that acute reduction in CSFP and acute rise in IOP may share similarities with respect to the damage on the optic nerve (Zhang et al., 2015).

Indeed, the pressure threshold of TLCPD is individually different, which is depending on the ONH geometry and the biomechanical properties of the tissues separating these compartments. Anatomically, the ONH separates the eye from the optic nerve surrounded by the subarachnoid space, forming a barrier between these two pressure compartments. Pressure changes in either compartment alter the pressure distribution across the ONH and hence the axial forces and transverse tension acting across the ONH. Previous investigation of ONH biomechanics has examined the effect of IOP alone on axial displacement of the lamina cribrosa. (Levy et al., 1981). However, a systematic evaluation of the effect of CSFP on ONH mechanics has not yet been reported.

In this work, we used finite element modeling to quantify low CSFP and high IOP-induced stresses and strains within the ONH. Our goal was to assess whether a low CSFP and a high IOP (especially a mild high IOP) resulting in same TLCPD will give rise to similar or different biomechanical responses of the optic nerve head. These results will help us better understand if a reduction in CSFP and an evaluation of IOP may have similar or different impact on the optic nerve head biomechanically.

RESULTS

A whole eye model with detailed ONH geometry was created (Figure 1). Figure 2 shows the undeformed shape of model (only tissue boundary lines are shown) at an IOP and CSFP of 0 mmHg and deformed shape of model (superimposed on the undeformed shape) at normal TLCPD of 10 mmHg and elevated TLCPD of 18 mmHg resulting by reduced CSFP or elevated IOP, at true scale (left) and with the deformation exaggerated six times (right). When TLCPD increases from 10 mmHg to 18 mmHg, pre-laminar neural tissue displaced laterally and posteriorly and LC had appreciable stretching, leading to the pre-laminar neural tissue and LC displaced backward and thinned. Comparatively, we observed higher deformations occurring at elevated TLCPD of 18 mmHg resulting by elevated IOP than by reduced CSFP.

The displacement patterns of the LC surfaces can be better understood by plotting the computed displacements as a function of position away from the center of the optic cup, as shown in Figure 3. The maximum LC posterior displacement occurred at the center of the cup, which is consistent with the results of Sigal et al. (2004). Also, the anterior surface of LC moved more than that of posterior surface of LC, leading to reduced thickness of LC. Moreover, LC thinned more at elevated IOP than by reduced CSFP. For example, at the center of the LC, thickness decreased by 6.2% caused by elevated IOP and 4.8% by reduced CSFP, at the same elevated TLCPD of 18 mmHg. To get a general understanding of how biomechanical response of the optic nerve head are affected by IOP, we set CSFP to normal 10 mmHg, and allowed IOP to vary from 20 mmHg to 50 mmHg. Figure 4 shows computed distributions of von Mises equivalent stress (left column) and 1st principal strain (right column), under an IOP varying from 20 mmHg to 50 mmHg. As IOP increased, we observed higher stresses and strains. The largest stresses were observed in the relatively stiff sclera and pia mater, compared with the relatively soft neural and laminar tissue. The largest strains were observed in the neural tissue around the sclera ring, which is directly related to the anatomical structure of ONH.

The nonmyelinated intraocular optic fibers traverse the outer layers of the retina, then the choroid, and finally the sclera and pass through the lamina cribrosa to become the intraorbital part of the optic nerve (Kozobolis et al., 2013). When these fibers traverse the sclera, the surrounding fibers are in direct contact with sclera. Under elevated IOP, the optic nerve at the level of the sclera ring bear the maximum strain, according to the model prediction. When IOP was elevated from 20 mmHg to 50 mmHg, both direct mechanic injury and other complex pathophysiological mechanisms may induce the pathological changes of axons. The maximum principle strains in this region suggested that the axons may be most vulnerable to mechanical insults. This appeared to agree with observations in the pattern of visual field defects in glaucomatous optic neuropathy (Quigley et al., 1982). The reduction of CSFP has a limited range and therefore does not generate a range of increase in TLCPD as large as that due to the elevation of IOP. To further assess how strains in the ONH are affected by mild increased of TLCPD resulted by reduced CSFP or mild elevated IOP, we first set CSFP to 10 mmHg, and allowed IOP to vary from 22 mmHg to 28 mmHg. Then we set IOP to 20 mmHg, and allowed CSFP to vary from 8 mmHg to 2 mmHg. We compared the different strains of ONH affected by a reduction in CSFP as well as a mild evaluation of IOP resulting in the

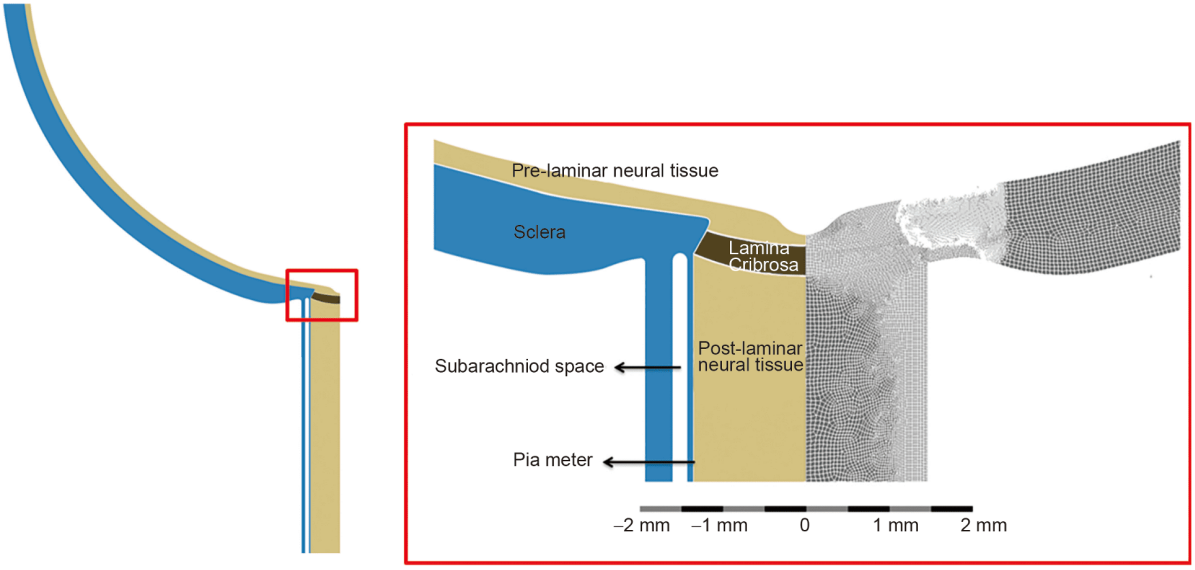

Figure 1 Model geometries and meshes. Left: details of the ONH region and a typical finite element mesh formed by eight-node quadrilaterals.

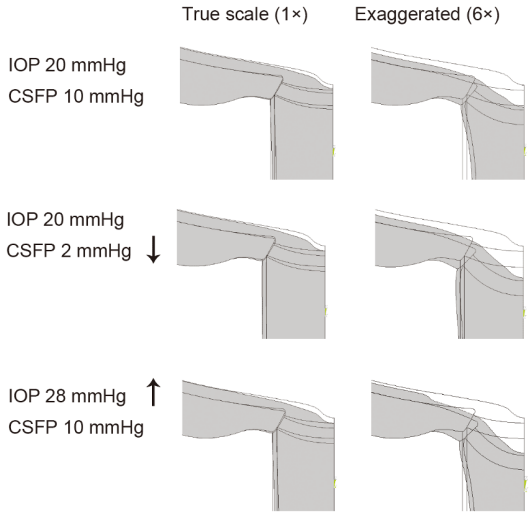

Figure 2 Shape change of the ONH at different combinations of IOP and CSFP. Left: true scale of the deformations; right: deformations exaggerated six times.

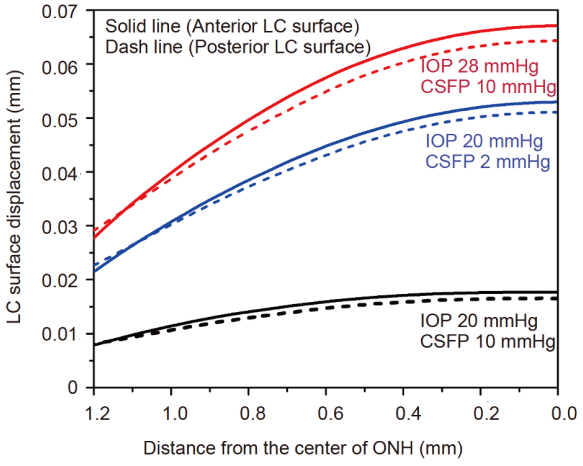

Figure 3 Computed displacement profiles of LC surfaces. Plots of LC displacement versus distance from center of the ONH as TLCPD increased from 10 mmHg to 18 mmHg resulted by elevated IOP or reduced CSFP. (Solid line) LC anterior surface; (Dash line) LC posterior surface.

same TLCPD. As shown in Figure 5, mild evaluation of IOP had an appreciable effect on strains within the LC. The effects of CSFP also have some effect on the strains of the ONH tissue, yet average peak strain within the lamina is relatively more defect by reduced CSFP than by mildly elevated IOP even at the same TLCPD.

The peak strains experienced in each region of ONH tissues are also summarized in Table 1. The results showed that reduced CSFP and elevated IOP leading to increased TLCPD were particularly influential. As TLCPD increased from 12 mmHg to 18 mmHg resulted by reduced CSFP or elevated IOP, there was a clear effect of increased TLCPD leading to larger peak tensile and compressive strains in the ONH tissue, including both prelamina neural tissue and laminar cribrosa. Also, we observed higher strains occurring at the pre-laminar neural tissue anterior to the LC than the post-laminar neural tissue.

More intuitive understanding of the difference between IOP and CSFP in the deformed shape of optic nerve head can be manifested by cup/disc (C/D) ratio. Figure 6 shows C/D ratio at different TLCPD. The red line is varying CSFP with IOP at 20 mmHg while the black line is varying IOP with CSFP at 10 mmHg. The result shows that, at the same TLCPD, low CSFP group exhibits less ONH deformation than those of the mildly high IOP group. For example, at an IOP of 20 mmHg, C/D averaged from 0.38 to 0.48 with reduced CSFP from 10 mmHg to 2 mmHg. At a CSFP of 10 mmHg, C/D averaged from 0.38 to 0.43 with elevated

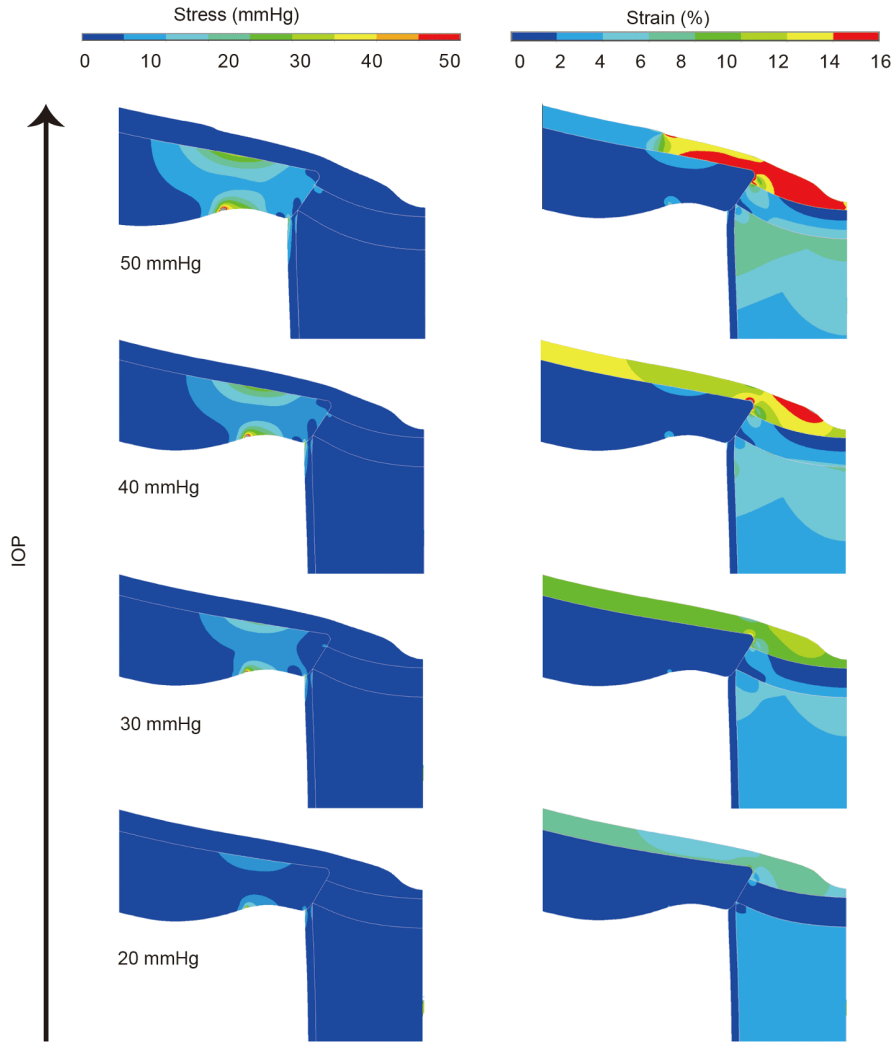

Figure 4 Stress and strain distributions. Contour plots of magnitude of computed distributions of von Mises equivalent stress (left) and 1st principal strain (right) in the ONH region at an CSFP of 10 mmHg and an IOP evaluated from 20 mmHg to 50 mmHg. The geometry is shown at true deformation scale.

IOP from 20 mmHg to 28 mmHg. In comparison, when the TLCPD is at 16 mmHg, C/D is 0.45 caused by elevated IOP while C/D is 0.42 caused by reduced CSFP.

DISCUSSION

Our goal was to understand how elevations in IOP and reduction in CSFP altered the biomechanical environment within the ONH, and to specifically identify the different biomechanical response of the optic nerve under the same TLCPD. This result is valuable for further understanding the different mechanisms implicated in the relationship between IOP or CSFP and the development of glaucomatous optic neuropathy, particularly at the level of the lamina cribrosa. The model suggests that biologically significant levels of strain are produced within the LC as the TLCPD goes from physiologic to elevated, even without considering the magnifying effects of the lamina's microarchitecture.

More generally, under elevated IOP conditions, ONH tissue would experience strains more extreme than would occur by reduced CSFP even at same TLCPD. IOP acts on the optic nerve head and the sclera by two force vectors. Firstly, the IOP is usually higher than other pressure around optic nerve tissue, generating an inside-out force. Secondly, the IOP generates a wall tension that pulls on the perimeter of the nerve head (Quigley et al., 1991). The tissues at this complex opening in the eye wall are specialized to account for these forces. Theoretically, CSFP in the retrobulbar space have the same effect as an increased IOP on the TLCPD. Orbital CSFP provides a radial stress for the optic nerve sheaths, an elevation in orbital CSFP causes an enlargement of the cerebrospinal fluid space around the optic nerve due to the principles of elasticity according to Poisson's effect. Under normal CSFP, the post-laminar neural is radially compressed, and thus expands anteriorly-posteriorly to push against the posterior LC. As CSFP decreased, the push will be diminished, resulting in an increase in strains within the lamina

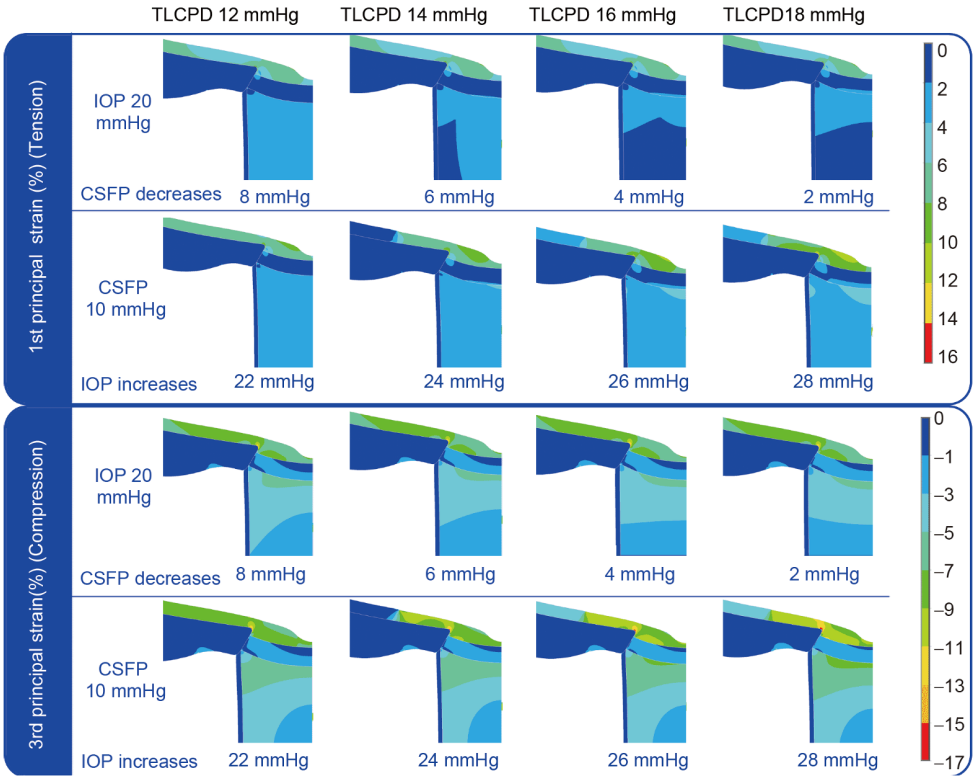

Figure 5 Computed 1st principal strain and 3rd principal strain in ONH tissues as TLCPD is varied from 12 mmHg to 18 mmHg resulted by reduced CSFP or elevated IOP. All other parameter values are assigned to the baseline values except IOP or CSFP. Specifically, when increase of TLCPD is resulted by reduced CSFP, IOP is set to 20 mmHg; when increase of TLCPD is resulted by elevated IOP, CSFP is set to 10 mmHg.

Table 1 The peak strains experienced in each region of ONH tissues as TLCPD is varied from 12 mmHg to 18 mmHg resulted by reduced CSFP or elevated IOP

Tissue Regions	Peak Strain	Pressure	TLCPD 12 mmHg	TLCPD 14 mmHg	TLCPD 16 mmHg	TLCPD 18 mmHg
pre-laminar neural tissue	Tension	CSFP↓	9.50	10.03	10.57	11.10
	Compression		−15.20	−15.61	−16.03	−16.44
	Tension	IOP↑	10.14	11.35	12.50	13.66
	Compression		−16.47	−18.18	−19.86	−21.55
lamina cribrosa	Tension	CSFP↓	4.71	5.17	5.63	6.09
	Compression		−2.65	−2.93	−3.21	−3.49
	Tension	IOP↑	4.91	5.61	6.25	6.91
	Compression		−2.75	−3.15	-3.52	−3.90
pos-tlaminar neural tissue	Tension	CSFP↓	3.37	3.14	3.10	3.18
	Compression		−5.75	−5.61	−5.50	−5.44
	Tension	IOP↑	3.85	4.07	4.32	4.57
	Compression		−6.41	−6.91	−7.43	−7.94
sclera	Tension	CSFP↓	2.58	2.82	3.05	3.29
	Compression		−4.48	−4.90	−5.33	−5.75
	Tension	IOP↑	2.70	2.88	3.29	3.63
	Compression		−4.67	−5.09	−5.78	−6.38

which can lead to tissue remodel (Feola et al., 2013; Majima et al., 2003; Nagels et al., 2003). Comparatively, larger peak strains by elevated IOP may cause more direct mechanical injury at the tissue and cellular level and influence the cellular phenotype than by decreased CSFP. Although the exact level of strain that leads to pathophysiology in the ONH is not known, there is some evidence that strains between 4% and 6% may lie outside the physiological loading range for

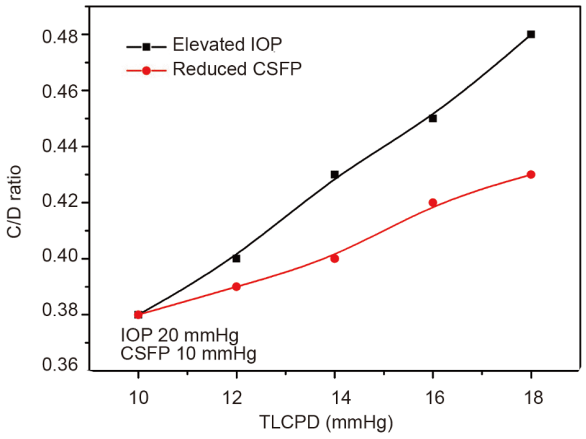

Figure 6 C/D ratios at different TLCPDs. The red line is reduced CSFP with IOP at 20 mmHg while the black line is mildly elevated IOP with CSFP at 10 mmHg.

ocular tissues and alter cellular phenotype(Beckel et al., 2014; Downs et al., 2003; Edwards and Good, 2001; Margulies and Thibault, 1992; Triyoso and Good, 1999; Yang et al., 2007).

Notably, under elevated IOP conditions, ONH would experience strain concentration in their neural and laminar regions, especially around the sclera ring. Because when optic nerve fibers traverse the sclera, the surrounding fibers are directly in contact with sclera. Based on our model prediction, under the action of mechanical forces caused by elevated IOP, the axons in close contact with the sclera ring would bear the maximum strain and may be the first to be injured.

In our model, elevating IOP increased the compressive strains experienced in the pre-laminar neural tissue and the lamina cribrosa, which could thus possibly initiate a cellular response in the ONH. However, reduced CSFP would cause smaller strain increase in preliminar and LC tissue, and thus may not induce cellular response

Band et al. (2009) suggested that the elevated IOP present in glaucoma is adequate to significantly impact intracellular axonal fluid flow. In the periphery of the optic nerve head, this flow may be sufficient to disrupt the diffusion of ATP and hence interrupt active axonal transport. A decrease in CSF pressure can also occur clinically, giving rise to an increased TLCPD. Our previous studies in a rat model have shown that an increase in TLCPD, caused by either an increase in IOP or a decrease in CSFP, could induce changes in the levels of the axonal transport (Zhang et al., 2015). Reduction in CSFP and elevation in IOP resulting in same TLCPD may induce different biomechanical responses in the optic nerve head, but similar changes in the levels of the axonal transport which produce a significant axial flux and an interruption of active axonal transport (Zhang et al., 2015).

In summary, reduction in CSFP and elevation in IOP resulting in same TLCPD induce different biomechanical responses in the optic nerve head. With acutely elevated IOP, the maximum principle strains resulted from IOP elevations were highest within the neural and laminar regions, especially around the sclera ring, reaching potentially biologically significant levels. Therefore, acutely elevated IOP, it is plausible that direct mechanical injury could contribute to glaucomatous optic neuropathy. While the reduction in CSFP lead to smaller strain increase in the optic nerve head at the same level of TLCPD as compared to increased IOP, indicating a potential role of low CSFP in the pathogenesis of glaucoma.

Our study has several potential limitations. First, the results in this study were obtained from simplified models, and naturally there are aspects of the biomechanics of the ONH that are not captured. Second, the tissues were modeled as linear-elastic and isotropic, whereas most soft biological tissues, such as the LC, display nonlinear and viscoelastic behavior and have a complex collagen matrix. Third, our model does not account for central retinal vessels which may have a mechanical effect on the deformation of the central region of the optic disc, acting like a tent pole (Jonas et al., 2001). Fourth, our model does not account for axoplasmic stasis that may contribute to swelling of pre-laminar neural tissue that is visible by OCT.

MATERIALS AND METHODS

Computational biomechanical simulation of ONH was performed with the ANSYS software (ANSYS 14.5, Inc, USA). Finite element method has been commonly applied in biomechanics due to its ability to handle complex geometries. (Roberts et al., 2010; Norman et al., 2011; Sigal, 2011). A whole eye model with detailed ONH geometry was created. Away from the ONH region, the sclera-corneal formed a spherical shell with a 0.78 mm thickness and a 12 mm internal radius (Olsen et al., 1998). In the ONH region, the sclera incorporated a tapered scleral canal, with an anterior opening of 1.52 mm diameter. The pre-laminar neural tissue included an optic cup and a prepapillary rim in the ONH region. The cup was shaped so that the cup-to-disc ratio was 0.33 when measured with respect to a level at 0.05 mm below the retina surface at the rim. The thickness of pia mater is 0.06 mm and the thickness of sclera varied from 0.46 mm at its thinnest point, adjacent to the canal, to 0.8 mm at 10° from the axis of symmetry (Sigal et al., 2004). The LC was modeled as a section of a spherical shell, concentric to the scleral-corneal shell, 0.3 mm thick with a 12.4 mm internal radius. The shortest distance between the anterior surface of the LC and the cerebrospinal fluid space was 0.39 mm and between the anterior surface of the LC and the pia mater was

0.28 mm. The latter value is within the ranges reported by Jonas et al (Jonas et al., 1988; Jonas and Budde, 2000; Jonas et al., 2003). The post-laminar optic nerve extended posteriorly from the LC and filled most of the scleral canal.

The mechanical properties of the tissues that constitute the ONH and surrounding structures have not been fully characterized. In this study, all materials were assumed to be linearly elastic, isotropic, and incompressible, in which case all that was needed to characterize the tissue's biomechanical behavior was the modulus of elasticity (Young's modulus). Moduli of 3 and 0.03 MPa were chosen for sclera and neural tissue, respectively. Mechanical modeling of the LC is complex. It is a composite of connective tissue with pores through which glial cells and nerve fibers pass. In this work we treated the LC as homogeneous, which implies that computed stresses and strains must be interpreted as mean values over an averaging region that is larger than several LC pores. It is expected that the LC should be stiffer than neural tissue but more compliant than sclera. Based on experimental tests with tissue strips, we estimated the Young's modulus for LC to be approximately 0.3 MPa (Edwards and Good, 2001). Zhivoderov has reported an elasticity modulus for pia mater between 1.44 and 4.65 MPa (Zhivoderov et al., 1983). We assigned the pia mater a Young's modulus of 3 MPa, the same as for the sclera. The mechanical properties of ONH tissue regions are summarized in Table 2.

A uniform IOP was applied to all interior surfaces of the eye—that is, the vitreoretinal interface and sclera-cornea anterior to the retinal termination. A range of IOPs from 10 mmHg to 50 mmHg was considered. External surfaces of the eye were subject to a pressure of 0 mmHg (relative to the atmospheric pressure). In addition to the IOP, the ONH is exposed to a hydrostatic pressure from the cerebrospinal fluid (CSFP). Specifically, CSFP was acted to the inner surface of the dura mater and external surface of the pia mater. We tested the effects of CSF pressures ranging from 2 mmHg to 10 mmHg. The boundary condition as that nodes on the equator and on the axis of symmetry are displacement constraint. The bottom margin of the model is fixed.

We used the maximum principal strain and von Mises equivalent stress. We used a value of 0.49 for poisson's ratio. For incompressible material, the maximum principal strains are nonnegative, always giving a measure of maximum extension. Von Mises equivalent stresses give an indication of the distortion energy acting throughout the tissue, while discounting the effects of hydrostatic pressure. Because of the linear elasticity assumption used in this model, all stresses and strains scale linearly with the applied loads.

Table 2 Mechanical properties of ONH tissues specified for pre-laminar neural tissue, lamina cribrosa, post-laminar neural tissue, sclera, and pia mater

Tissue Regions	Young's Modulus (MPa)
pre-laminar neural tissue	0.03
lamina cribrosa	0.3
post-laminar neural tissue	0.03
sclera	3
pia mater	3

Compliance and ethics *The author(s) declare that they have no conflict of interest.*

Acknowledgements *This work was supported by the National Natural Science Foundation of China (81271005, 81300767), the Beijing Natural Science Foundation (7122038, 7162037), and the Basic-Clinical Research Cooperation Funding of Capital Medical University (2016-JLPT-Y03). The funders had no role in study design, data collection and analysis, decision to publish, or preparation of the manuscript.*

References

Band, L.R., Hall, C.L., Richardson, G., Jensen, O.E., Siggers, J.H., and Foss, A.J.E. (2009). Intracellular flow in optic nerve axons: A mechanism for cell death in glaucoma. Invest Ophthalmol Vis Sci 50, 3750–3758.

Beckel, J.M., Argall, A.J., Lim, J.C., Xia, J., Lu, W., Coffey, E.E., Macarak, E.J., Shahidullah, M., Delamere, N.A., Zode, G.S., et al. (2014). Mechanosensitive release of adenosine 5'-triphosphate through pannexin channels and mechanosensitive upregulation of pannexin channels in optic nerve head astrocytes: A mechanism for purinergic involvement in chronic strain. Glia 62, 1486–1501.

Berdahl, J.P., Allingham, R.R., and Johnson, D.H. (2008). Cerebrospinal fluid pressure is decreased in primary open-angle glaucoma. Ophthalmology 115, 763–768.

Downs, J.C., Suh, J.K.F., Thomas, K.A., Bellezza, A.J., Burgoyne, C.F., and Hart, R.T. (2003). Viscoelastic characterization of peripapillary sclera: Material properties by quadrant in rabbit and monkey eyes. J Biomech Eng 125, 124–131.

Edwards, M.E., and Good, T.A. (2001). Use of a mathematical model to estimate stress and strain during elevated pressure induced lamina cribrosa deformation. Curr Eye Res 23, 215–225.

Feola, A., Abramowitch, S., Jallah, Z., Stein, S., Barone, W., Palcsey, S., and Moalli, P. (2013). Deterioration in biomechanical properties of the vagina following implantation of a high-stiffness prolapse mesh. BJOG 120, 224–232.

Geijssen, H.C. (1991). Studies on Normal Pressure Glaucoma. Amsterdam: Kugler Publication.

Jonas, J.B., Gusek, G.C., Guggenmoos-Holzmann, I., and Naumann, G.O.H. (1988). Size of the optic nerve scleral canal and comparison with intravital determination of optic disc dimensions. Graefe's Arch Clin Exp Ophthalmol 226, 213–215.

Jonas, J.B., and Budde, W.M. (2000). Diagnosis and pathogenesis of glaucomatous optic neuropathy: Morphological aspects. Prog Retinal Eye Res 19, 1–40.

Jonas, J.B., Budde, W.M., Németh, J., Gründler, A.E., Mistlberger, A., and Hayler, J.K. (2001). Central retinal vessel trunk exit and location of glaucomatous parapapillary atrophy in glaucoma. Ophthalmology 108, 1059–1064.

Jonas, J.B., Berenshtein, E., and Holbach, L. (2003). Anatomic relationship between lamina cribrosa, intraocular space, and cerebrospinal fluid space. Invest Ophthalmol Vis Sci 44, 5189–5195.

Kozobolis, V., Konstantinidis, A., and Labiris, G. (2013). Recognizing a glaucomatous optic disc. In: Rumelt, S., ed. Glaucoma-Basic and Clinical Aspects. 749–750.

Levy, N.S., Crapps, E.E., and Bonney, R.C. (1981). Displacement of the optic nerve head. Arch Ophthalmol 99, 2166–2174.

Liu, L., Li, X., Killer, H.E., Cao, K., Li, J., and Wang, N. (2019). Changes in retinal and choroidal morphology after cerebrospinal fluid pressure reduction: A Beijing iCOP study. Sci China Life Sci 62, 268–271.
Morgan, W.H., Chauhan, B.C., Yu, D.Y., Cringle, S.J., Alder, V.A., and House, P.H. (2002). Optic disc movement with variations in intraocular and cerebrospinal fluid pressure. Invest Ophthalmol Vis Sci 43, 3236–3242.
Morgan, W.H., Yu, D.Y., and Balaratnasingam, C. (2008). The role of cerebrospinal fluid pressure in glaucoma pathophysiology: The dark side of the optic disc. J Glaucoma 17, 408–413.
Majima, T., Yasuda, K., Tsuchida, T., Tanaka, K., Miyakawa, K., Minami, A., and Hayashi, K. (2003). Stress shielding of patellar tendon: Effect on small-diameter collagenfibrils in a rabbit model. J Orthop Sci 8, 836–841.
Margulies, S.S., and Thibault, L.E. (1992). A proposed tolerance criterion for diffuse axonal injury in man. J Biomech 25, 917–923.
Nagels, J., Stokdijk, M., and Rozing, P.M. (2003). Stress shielding and bone resorption in shoulder arthroplasty. J Shoulder Elbow Surg 12, 35–39.
Norman, R.E., Flanagan, J.G., Sigal, I.A., Rausch, S.M.K., Tertinegg, I., and Ethier, C.R. (2011). Finite element modeling of the human sclera: Influence on optic nerve head biomechanics and connections with glaucoma. Exp Eye Res 93, 4–12.
Olsen, T.W., Aaberg, S.Y., Geroski, D.H., and Edelhauser, H.F. (1998). Human sclera: Thickness and surface area. Am J Ophthalmol 125, 237–241.
Quigley, H.A., Addicks, E.M., and Green, W.R. (1982). Optic nerve damage in human glaucoma. Arch Ophthalmol 100, 135.
Quigley, H.A., Brown, A., and Dorman-Pease, M.E. (1991). Alterations in elastin of the optic nerve head in human and experimental glaucoma. British J Ophthalmol 75, 552–557.
Ren, R., Wang, N., Zhang, X., Cui, T., and Jonas, J.B. (2011). Trans-lamina cribrosa pressure difference correlated with neuroretinal rim area in glaucoma. Graefes Arch Clin Exp Ophthalmol 249, 1057–1063.
Roberts, M.D., Liang, Y., Sigal, I.A., Grimm, J., Reynaud, J., Bellezza, A., Burgoyne, C.F., and Downs, J.C. (2010). Correlation between local stress and strain and lamina cribrosa connective tissue volume fraction in normal monkey eyes. Invest Ophthalmol Vis Sci 51, 295–307.
Sigal, I.A., Flanagan, J.G., Tertinegg, I., and Ethier, C.R. (2004). Finite element modeling of optic nerve head biomechanics. Invest Ophthalmol Vis Sci 45, 4378–4387.
Sigal, I.A. (2011). An applet to estimate the IOP-induced stress and strain within the optic nerve head. Invest Ophthalmol Vis Sci 52, 5497–5506.
Triyoso, D.H., and Good, T.A. (1999). Pulsatile shear stress leads to dna fragmentation in human SH-SY5Y neuroblastoma cell line. J Physiol 515, 355–365.
Wang, N., Xie, X., Yang, D., Xian, J., Li, Y., Ren, R., Peng, X., Jonas, J.B., and Weinreb, R.N. (2012). Orbital cerebrospinal fluid space in glaucoma: The Beijing intracranial and intraocular pressure (iCOP) study. Ophthalmology 119, 2065–2073.e1.
Yang, D., Fu, J., Hou, R., Liu, K., Jonas, J.B., Wang, H., Chen, W., Li, Z., Sang, J., Zhang, Z., et al. (2014). Optic neuropathy induced by experimentally reduced cerebrospinal fluid pressure in monkeys. Invest Ophthalmol Vis Sci 55, 3067–3073.
Yang, H., Downs, J.C., Bellezza, A., Thompson, H., and Burgoyne, C.F. (2007). 3-D histomorphometry of the normal and early glaucomatous monkey optic nerve head: Prelaminar neural tissues and cupping. Invest Ophthalmol Vis Sci 48, 5068–5084.
Zhang, Z., Liu, D., Jonas, J.B., Wu, S., Kwong, J.M.K., Zhang, J., Liu, Q., Li, L., Lu, Q., Yang, D., et al. (2015). Axonal transport in the rat optic nerve following short-term reduction in cerebrospinal fluid pressure or elevation in intraocular pressure. Invest Ophthalmol Vis Sci 56, 4257–4266.
Zhivoderov, N.N., Zavalishin, N.N., and Neniukov, A.K. (1983). Mechanical properties of the dura mater of the human brain. Sudebno-meditsinsk Ekspert 26, 36–37.